ORIGINAL RESEARCH

Hypotension Due to Kir6.1 Gain-of-Function in Vascular Smooth Muscle

Anlong Li, MD, PhD; Russell H. Knutsen, BS; Haixia Zhang, MD, PhD; Patrick Osei-Owusu, PhD; Alex Moreno-Dominguez, PhD; Theresa M. Harter, BS; Keita Uchida, BS; Maria S. Remedi, PhD; Hans H. Dietrich, PhD; Carlos Bernal-Mizrachi, MD; Kendall J. Blumer, PhD; Robert P. Mecham, PhD; Joseph C. Koster, PhD;† Colin G. Nichols, PhD

***Background*—**K_{ATP} channels, assembled from pore-forming (Kir6.1 or Kir6.2) and regulatory (SUR1 or SUR2) subunits, link metabolism to excitability. Loss of Kir6.2 results in hypoglycemia and hyperinsulinemia, whereas loss of Kir6.1 causes Prinzmetal angina–like symptoms in mice. Conversely, overactivity of Kir6.2 induces neonatal diabetes in mice and humans, but consequences of Kir6.1 overactivity are unknown.

***Methods and Results*—**We generated transgenic mice expressing wild-type (WT), ATP-insensitive Kir6.1 [Gly343Asp] (GD), and ATP-insensitive Kir6.1 [Gly343Asp,Gln53Arg] (GD-QR) subunits, under Cre-recombinase control. Expression was induced in smooth muscle cells by crossing with smooth muscle myosin heavy chain promoter–driven tamoxifen-inducible Cre-recombinase (SMMHC-Cre-ER) mice. Three weeks after tamoxifen induction, we assessed blood pressure in anesthetized and conscious animals, as well as contractility of mesenteric artery smooth muscle and K_{ATP} currents in isolated mesenteric artery myocytes. Both systolic and diastolic blood pressures were significantly reduced in GD and GD-QR mice but normal in mice expressing the WT transgene and elevated in Kir6.1 knockout mice as well as in mice expressing dominant-negative Kir6.1 [AAA] in smooth muscle. Contractile response of isolated GD-QR mesenteric arteries was blunted relative to WT controls, but nitroprusside relaxation was unaffected. Basal K_{ATP} conductance and pinacidil-activated conductance were elevated in GD but not in WT myocytes.

***Conclusions*—**K_{ATP} overactivity in vascular muscle can lead directly to reduced vascular contractility and lower blood pressure. We predict that gain of vascular K_{ATP} function in humans would lead to a chronic vasodilatory phenotype, as indeed has recently been demonstrated in Cantu syndrome. **(*J Am Heart Assoc.* 2013;2:e000365 doi: 10.1161/JAHA.113.000365)**

Key Words: hypotension • K_{ATP} • KCNJ8 • mice • transgenic • ABCC9

K_{ATP} channels were first reported in cardiac myocytes[1] and subsequently identified in pancreatic β cells, skeletal muscle, vascular smooth muscle (VSM),[2,3] and the central nervous system. K_{ATP} channels act as metabolic molecular sensors, being inhibited by ATP, and activated by MgADP.[4] Two inward rectifier potassium channel (Kir) genes, Kir6.1 (*KCNJ8*) and Kir6.2 (*KCNJ11*), encode the pore-forming subunits of the K_{ATP} channel, and 2 ATP-binding cassette (ABC) genes, SUR1 (*ABCC8*) and SUR2 (*ABCC9*), encode obligate regulatory subunits. The Kir6 proteins exhibit distinct nucleotide sensitivities[5] as well as distinct but overlapping tissue distributions.[6] Kir6.2 generates K_{ATP} channels in striated muscle, pancreas, and certain neuronal tissues, whereas Kir6.1 predominantly generates channels in VSM cells (VSMCs) and endothelial cells.

In the pancreatic β cell, K_{ATP} channels represent the central link between metabolism and the triggering of insulin secretion. Loss-of-function (LOF) mutations of Kir6.2 (or SUR1) results in congenital hyperinsulinism in humans, and essential features are replicated in Kir6.2 (or SUR1) knockout[7] or dominant-negative transgenic[8] mice. Conversely, Kir6.2 (or SUR1) gain-of-function (GOF) mutations underlie neonatal diabetes,[9] and the human disease was actually predicted by studies of Kir6.2 GOF transgenic mice.[10] Less is known about the disease

From the Departments of Cell Biology and Physiology (A.L., R.H.K., H.Z., P.O.-O., T.M.H., K.U., M.S.R., K.J.B., R.P.M., J.C.K., C.G.N.) and Neurological Surgery (H.H.D.), Center for the Investigation of Membrane Excitability Diseases (A.L., H.Z., A.M.-D., T.M.H., K.U., M.S.R., C.G.N.), and Division of Endocrinology, Department of Medicine (C.B.-M.), Washington University School of Medicine, St Louis, MO.

†Deceased.

Dr. Moreno-Dominguez is currently located at the Department of Physiology and Pharmacology, University of Calgary, Calgary, Alberta, Canada.

Dr. Anlong Li is currently located at the Vascular Research Laboratory, Providence VA Medical Center, Providence, RI

Correspondence to: Colin G. Nichols, PhD, Department of Cell Biology and Physiology, Campus Box 8228, 660 S Euclid Ave, St Louis, MO 63110. E-mail: cnichols@wustl.edu

Received June 12, 2013; accepted July 30, 2013.

relevance of Kir6.1. The only animal models of genetically modified Kir6.1 are the Kir6.1 knockout (Kir6.1$^{-/-}$) mouse[11] and the partial LOF (dominant-negative) Cx1-Kir6.1[AAA] mouse.[12] These animals implicate a role of Kir6.1 and the partner SUR2B subunit in the vascular system, specifically in control of coronary artery contractility and systemic blood pressure, and these mice, together with SUR2 knockout animals, reiterate a Prinzmetal angina and hypertensive phenotype,[11–13] explainable by loss of K_{ATP} somewhere within the vascular system. There are also several reports that cardiac early repolarization syndrome (ERS) is associated with Kir6.1 gene variants that may generate GOF channels,[14–16] although the relevant location of Kir6.1 in this case is unknown.

To date, there is no animal model available in which to further probe the potential in vivo role of Kir6.1 GOF. Given the high sequence homology between Kir6.1 and Kir6.2, we hypothesized that GOF mutations homologous to those in Kir6.2 that cause neonatal diabetes would have parallel pathological effects if present in Kir6.1. To address this, we have engineered mutations in Kir6.1 homologous to those that cause GOF in Kir6.2 and then generated novel Kir6.1 GOF transgenic mice that express these constructs as well as wild-type (WT) constructs under tamoxifen-inducible Cre-recombinase control. These mice permit the selective induction of transgene expression in any tissue of interest, thereby modeling tissue-specific expression of mutations. By crossing with SMMHC-Cre-ER) mice,[17] we have targeted the transgene to smooth muscle cells. Within 3 weeks after tamoxifen injection, both ATP-insensitive Kir6.1 [Gly343Asp] (GD)/Cre double-transgenic (DTG) and ATP-insensitive Kir6.1 [Gly343Asp, Gln53Arg] (GD-QR)/Cre DTG mutation mice develop a significant hypotensive phenotype, as a result of enhanced K^+ conductance and reduced contractility in VSM. In contrast, both blood pressure and K^+ conductance are unaffected in WT/Cre DTG animals, whereas blood pressure was elevated in Kir6.1[AAA]/Cre DTG and Kir6.1$^{-/-}$ animals. The results have important implications for understanding the consequence of Kir6.1 channel GOF in vivo and provide important hints for exploring the genetic and translational relevance in humans, providing a potential model for human Cantu syndrome, a multiorgan disease now shown to result from SUR2 GOF mutations.

Materials and Methods

Mutation and Expression of K_{ATP} Channels in COSm6 Cells

Point mutations ([Gly343Asp], [Gln53Arg]) were prepared using the Stratagene Quickchange kit, in rat Kir6.1 cDNA. COSm6 cells were transfected with pCDNA3-Kir6.1 (Kir6.1 WT, Kir6.1 [Gly343Asp], Kir6.1 [Gln53Arg]), pcDNA3-SUR1, and green fluorescent protein using FuGENE 6 Transfection Reagent (Promega). After transfection, cells were cultured for 48 hours, and excised patch-clamp experiments were made at room temperature using a perfusion chamber that allowed for the rapid switching of solutions. Data were typically filtered at 1 kHz, digitized at 5 kHz, and stored directly on a computer hard drive using Clampex software (Molecular Devices). The standard pipette (extracellular) and bath (cytoplasmic) solution used in these experiments had the following composition (in mmol/L): KCl 140, EGTA 1, K_2-EDTA 1, and K_2HPO_4 4, pH 7.3.

^{86}Rubidium Efflux

$^{86}Rb^+$ efflux was used to assay transport through K_{ATP} channels. COSm6 cells were grown and transfected in 12-well plates. Twenty-four hours after transfection, cells were incubated overnight at 37°C in DMEM containing ^{86}RbCl 0.05 MBq/mL. The medium was then aspirated and incubated cells were washed 3× with Ringer's solution (in mmol/L: HEPES 10, NaCl 118, $NaHCO_3$ 25, KCl 4.7, KH_2PO_4 1.2, $CaCl_2$ 2.5, $MgSO_4$ 1.2, adjusted to pH 7.4 with NaOH), and incubated for 15 minutes with 1 mL of Ringer's solution with or without metabolic inhibitors, Oligomycin 2.5 mg/mL and 2-deoxy-D-glucose 1 mmol/L at room temperature. After incubation, the supernatant was aspirated into vials, scintillation fluid was added for counting (4 mL to each vial), and new Ringer's solution was immediately added to the well. This step was repeated to time points 2.5, 5, 7.5, 15, 25, and 40 minutes, and 2% SDS was added to lyse the cells, which were assayed for remaining Rb content. Radioactivity in the supernatant and cell lysates was counted and efflux was expressed as a percentage of the total amount of radioactivity initially loaded into the cells.

Generation of CX1-Kir6.1 WT, GD, and GD-QR Transgenic Mice

All procedures complied with the standards for the care and use of animal subjects as stated in the "Guide for the Care and Use of Laboratory Animals" (National Institutes of Health, revised 2011) and were reviewed and approved by the Washington University Animal Care and Use Committee. Rat and mouse Kir6.1 differ in only 2 amino acids (of 424), and inducible Kir6.1 transgenes were generated by subcloning rat WT Kir6.1 as well as Kir6.1[Gly343Asp] and Kir6.1[Gly343Asp, Gln53Arg] cDNAs downstream of the CX-1 promoter in the pBS-CX1-LEL vector (a gift from Dr Gary Owens, University of Virginia), which contains the chicken β-actin (CX1) promoter followed by the enhanced green fluorescent protein coding region (including a stop codon), flanked by 2 loxP sites, to create CX1-Kir6.1, CX1-Kir6.1[Gly343Asp], and CX1-Kir6.1 [Gly343Asp,Gln53Arg] transgenic constructs. The expression

cassette was excised by enzyme digestion, purified, and microinjected into fertilized eggs of C57Bl6xCBA mice, according to standard techniques, in the Washington University Neuroscience Transgenic Facility. Transgenic mice were identified by the use of PCR on mouse-tail DNA using green fluorescent protein–specific oligonucleotide primers. Six to 11 founder mice carrying WT, GD, or GD-QR were identified and bred to homogeneity by multiple (6×) back-crossing to C57Bl6 mates. Of the founder mice that were generated, the lines with highest expression were WT line 1 and line 2, GD line 9 and line 10, and GD-QR line 1 and line 2. Accordingly, analysis was concentrated on these high-expressing animals, and all presented data are from these animals.

Blood Pressure Measurements

In Anesthetized Animals

Animals were anesthetized using inhaled isoflurane and restrained on a heated holder to maintain body temperature. A Millar pressure transducer was carefully inserted into the right carotid artery and moved to the ascending aorta, where baseline heart rate, systolic, diastolic, and mean blood pressures were monitored. All measurements were obtained under 1% isoflurane anesthesia. Systolic, diastolic, and mean blood pressures and heart rate were calculated using Chart 5 for Windows software.

In Conscious Animals

Systolic blood pressure, diastolic blood pressure, and mean blood pressure were also measured in conscious mice using a tail-cuff system (Kent Scientific) as previously described.[18] Animals were acclimated to handling and placement in the apparatus daily for 2 weeks before the measurement of blood pressure. Multiple measurements were made at each of 3 daily sessions and averaged to obtain a single value for each mouse.

Tissue Preparation and Smooth Muscle Cell Isolation

Adult mice were anesthetized with Avertin (Sigma-Aldrich), and aortas and mesenteric arteries were rapidly removed and placed in ice-cold HEPES-buffered PSS containing (in mmol/L) NaCl 134, KCl 6, $CaCl_2$ 2, $MgCl_2$ 1, HEPES 10, and glucose 10, with pH adjusted to 7.4 with NaOH. For molecular biology experiments, the mesenteric arteries and the aortas were dissected, cleaned to remove adventitial connective tissue, and were kept in a −80°C freezer until use. For patch-clamp experiments, individual smooth muscle cells were enzymatically dissociated from mesenteric arteries in isolation solution of the following composition (in mmol/L): NaCl 55, sodium glutamate 80, KCl 5.6, $MgCl_2$ 2, HEPES 10, and glucose 10, pH 7.3 with NaOH, and then placed into isolation solution containing papain 12.5 μg/mL, dithioerythreitol 1 mg/mL, and BSA 1 mg/mL for 10 minutes (at 37°C), and then immediately transferred to isolation solution containing collagenase (type H:F=1:2) 1 mg/mL, $CaCl_2$ 100 μmol/L, and BSA 1 mg/mL for 8 minutes (at 37°C). Arteries were subsequently washed in ice-cold isolation solution for 10 minutes and triturated using a polished glass Pasteur pipette to yield single smooth muscle cells. Cells were stored on ice and used for electrophysiology experiments between 1 and 8 hours after isolation. For primary culture of VSMCs, the procedures were as follows: Arteries were isolated and cleaned free of connective tissue. The endothelium was removed by gently rubbing the luminal surface with a cotton swab. Arteries were then digested as just described—for step 1, aorta for 30 minutes and mesenteric artery for 20 minutes, and for step 2, aorta for 10 minutes and mesenteric artery for 7 minutes. Smooth muscle cells were gently dispersed via trituration with a small-bore pipette in Ca^{2+}-free HBSS at room temperature. The dispersed cells were cultured at 37°C and 5% CO_2 in DMEM/F-12 medium (with L-glutamine) supplemented with 10% fetal bovine serum, streptomycin 100 U/mL, and penicillin 0.1 mg/mL for 3 to 5 days before use.

Whole-Cell Patch-Clamp Electrophysiology

Freshly isolated mesenteric artery smooth muscle cells were allowed to adhere to a glass coverslip in the bottom of the recording chamber for 10 minutes before experimentation. K_{ATP} currents were measured using the whole-cell configuration of the patch-clamp technique with an Axopatch 700B amplifier (Molecular Devices) at holding potential −70 mV. The bath solution was HEPES-buffered PSS containing (in mmol/L) KCl 140 (or KCl 6 plus NaCl 136), $CaCl_2$ 2, $MgCl_2$ 1, HEPES 10, and glucose 10, with pH adjusted to 7.4 with KOH (or NaOH). The pipette solution contained (in mmol/L) potassium aspartate 110, KCl 30, NaCl 10, $MgCl_2$ 1, HEPES 10, $CaCl_2$ 0.5, K_2HPO_4 4, and EGTA 5, with pH adjusted to 7.2 with KOH. Membrane currents were filtered at 1 kHz and digitized at 4 kHz.

Total RNA Extraction, cDNA Synthesis, and Quantitative Real-Time PCR

Arteries were mechanically homogenized, and total RNA was extracted using a commercial kit (Qiagen). After removal of contaminating DNA (Qiagen), RNA content was determined by NanoDrop 1000 (Thermo Scientific). Total RNA (0.5 μg) was used for first-strand cDNA synthesis with random primers and Superscript III RNase H^- reverse transcriptase (Invitrogen) according to the manufacturer's protocol. Primers for PCR

were designed to regions specific for rat Kir6.1 by primer 3 online software (sense: TGTGACCAATGTCAGGTCATTCACTTC; antisense: TGATGATCAGACCCACAATGTTCTGC); β-actin control primers were obtained from Sigma. At least 1 of each primer pair was designed to span exon–exon junctions, to minimize the possibility of amplifying genomic DNA. RT-PCR was carried out for 30 cycles using Platinum*Taq* DNA polymerase (Invitrogen), which involved denaturation at 94°C for 30 seconds, annealing at 55°C for 45 seconds, and extension at 72°C for 90 seconds, followed by a final extension at 72°C for 10 minutes, and the products were then stored at 4°C. PCR products were analyzed by electrophoresis with 1.8% agarose gel and visualized by ethidium bromide staining to optimize the primer for real-time PCR. Real-time PCRs were detected by use of SYBR Green and were performed with ABI Prism 7000 (Applied Biosystems), using 1 μL of cDNA as template in each 20-μL reaction mixture. The PCR protocol consisted of initial enzyme activation at 95°C for 5 minutes, followed by 40 cycles at 95°C for 15 seconds, and at 60°C for 1 minute. To confirm the specificity of PCR products, we obtained a melting curve at the end of each run by slow heating with increments of 0.5°C/10 seconds from 60° to 95°C, with fluorescence detected at intervals of 0.5°C. Standard gel electrophoresis was also performed to ensure the end product generated a single band with the predicted size (100 to 150 bases). Following baseline correction, a fluorescence threshold was established and the cycle when this threshold was crossed (C_t) was determined for each reaction. To control for variability in RNA quantity, the normalized value, ΔC_t, for each sample was calculated by using the formula $\Delta C_t = C_{t(actin)} - C_{t(kir6.1)}$. Relative expression in TG tissue (normalized to WT) was then determined using the following relationship: relative gene expression$=2^{-\Delta\Delta Ct}$, where $\Delta\Delta C_t = \Delta C_t$ (WT) $- \Delta C_t$ (TG).

Vessel Contractility and Reactivity Measurements

Male mice were anesthetized with ketamine (87 mg/kg IP) and xylazine (13 mg/kg IP). The small intestine was accessed after the abdomen was shaved and a midline incision was made, first through the skin and then through the abdominal muscle. The entire intestine was excised and placed in chilled 1% albumin in PSS (MOPS, pH 7.4) containing (in mmol/L) NaCl 144, KCl 3.0, $CaCl_2$ 2.5, $MgSO_4$ 1.5, pyruvate 2.0, glucose 5.0, EDTA 0.02, and NaH_2PO_4 1.21. The mouse was then killed via cervical dislocation. With use of a pair of fine forceps and with the aid of a dissecting microscope, adipose tissue was carefully removed from second order mesenteric arteries. Sections of isolated vessels 2 to 3 mm in length were excised and immediately placed in an organ chamber for mounting onto glass pipettes.

An excised piece of mesenteric artery was transferred into the organ chamber (2.5 mL vol) containing MOPS and mounted on the stage of an inverted microscope (Zeiss Axiovert S100TV). The vessel was cannulated on one end with a glass perfusion pipette and occluded on the other end with a collecting pipette such that no luminal flow was allowed during the experiment, and the lumen of the vessel filled with 1% albumin in MOPS buffer. The vessel was observed with a video camera system (MTI CCD-72) to track and record changes in vessel diameter in response to vasoactive agents. Baseline internal diameter of the vessel was measured online at 60 mm Hg and 37°C, with a computerized diameter tracking system (sampling rate of 10 Hz, Diamtrak 3 Plus; Montech Pty, Ltd). Vessel diameter in the presence of various vasoactive agents was measured after at least 30 minutes' equilibration, when the bath solution was replaced with warmed MOPS buffer containing freshly prepared solution.

For vessel reactivity assays, excised pieces of mesenteric artery were transferred and cannulated under no-flow condition in an organ bath. After vessels were equilibrated for 30 minutes, the bath solution was replaced with warmed MOPS containing increasing concentrations of phenylephrine (PE), and changes in vessel diameter were continuously recorded. To determine the effects of K_{ATP} channel blockade on PE-induced vasoconstriction, cannulated vessels were further incubated with glibenclamide 10 μmol/L for 10 minutes before performing dose-response experimentd with PE as described. For K_{ATP} channel activation, PE dose-response was assessed in the presence of pinacidil 100 μmol/L. For vasodilatation experiments, vessels were constricted with PE 5 μmol/L after 30 minutes of equilibration at 37°C. After constriction had reached steady state (>1 minute), the bath solution was changed to MOPS containing PE 5 μmol/L and the endothelium-independent vasodilator sodium nitroprusside at various concentrations (10^{-9} to 10^{-4} mmol/L). After the highest sodium nitroprusside concentration was applied, the bath solution was replaced with MOPS to allow complete vessel relaxation back to control values.

Statistical Analysis

Unless otherwise stated, values are given as mean±SE; n values refer to the number of events analyzed. Student's *t* tests were used for comparison of unpaired data. For comparison between multiple data sets, we applied 1-way ANOVA followed by post-hoc Tukey's test or 2-way ANOVA followed by Bonferroni's posttests. When the sample size was ≤3, statistical analysis was not performed and significance is not assigned. Unless stated otherwise, asterisks in figures indicate significant difference (*P<0.05, **P<0.01) between the test group and the control group within time point or condition; nonsignificant differences are not indicated.

Chemicals

Papain was purchased from Worthington Biochemical. Unless otherwise stated, all other chemicals were obtained from Sigma Chemical.

Results

Predicted Kir6.1 GOF Mutations Reduce Channel ATP Sensitivity and Enhance Channel Activity in Intact Cells

Kir6.1 has high homology to Kir6.2, and most Kir6.2 mutations identified as causal in neonatal diabetes are at conserved residues. We generated Kir6.1[Gln53Arg] (Q53R, QR) and Kir6.1[Gly343Asp] (G343D, GD) single mutants (Figure 1A, equivalent to diabetes-causing Kir6.2 GOF mutations Gly334Asp[19] and Gln52Arg[20]), as well as Kir6.1[G343D, Q53R] (GD-QR) double mutants, and examined channel activity of these constructs in recombinant expression with sulfonylurea receptor subunits. In contrast to Kir6.2, Kir6.1 channels require the presence of Mg-nucleotides for significant channel activity, even though channels are sensitive to inhibition by ATP (Figure 1B), resulting in a biphasic dependence of channel activity on MgATP.[5] As shown in Figure 1B, WT Kir6.1 channels are stimulated up to ≈1 mmol/L MgATP and strongly inhibited at 10 mmol/L. In contrast, MgUDP stimulates channels but has no inhibitory effect (Figure 1B). Each of the mutant channels is activated similar to WT, but each shows reduced inhibition by MgATP, and there is an approximately additive effect in the GD-QR double mutant (Figure 1C). Reduced sensitivity to ATP inhibition is expected to result in enhanced channel activity in intact cells, and this is confirmed by $^{86}Rb^{+}$ flux experiments on intact cells, which show larger $^{86}Rb^{+}$ fluxes from intact cells expressing

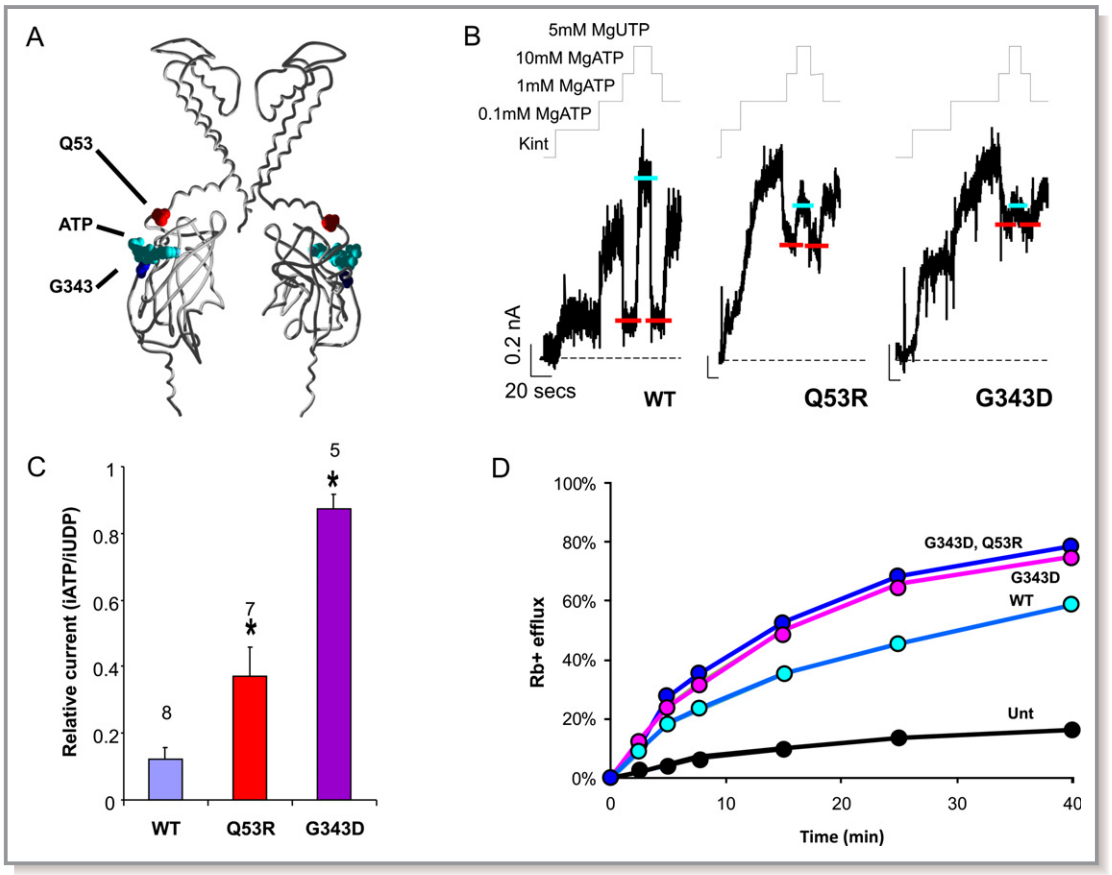

Figure 1. Reiteration of GOF phenotype from mutations in Kir6.1. A, Homology model of kir6.1 indicating location of mutated residues. Residue Gly343 is found in the predicted ATP binding site, whereas Gln53 is located in the amino-terminus and is involved in transduction. B, Excised patch currents from SUR1/Kir6.1 subunits coexpressed in COSm6 cells, in nucleotide-free Kint solution or in Mg-nucleotides as indicated. WT channels are activated at low [ATP] and high [UTP]. WT channels become strongly inhibited at high (10 mmol/L) ATP, but Gln53Arg (Q53R) and Gly343Asp (G343D) are insensitive to ATP inhibition. C, Averaged data from experiments as in (B) (currents in 10 mmol/L MgATP/current in 5 mmol/L MgUTP, mean±SEM, n as indicated, 1-way ANOVA followed by post-hoc Tukey's test). D, Representative data from an ^{86}Rb efflux experiment on untransfected (Unt) COS-m6 cells and cells transfected with Kir6.1WT, (G343D) or G343D, Q53R mutant channels, plus SUR1. Basal activity of GD or GD-QR channels was significantly higher than WT in the intact cell. GOF indicates gain-of-function; WT, wild-type.

[Gly343Asp] and [Gly343Asp, Gln53Arg] mutants than cells expressing WT channels, under basal conditions (Figure 1D).

Expression of Kir6.1 GOF in Smooth Muscle Cells

In order to study the effects of Kir6.1 GOF in vivo, we have generated transgenic mice that express WT, GD, or GD-QR mutant Kir6.1 constructs under tamoxifen-inducible Cre-recombinase control in the pBS-CX1-LEL vector. The transgenic animals express green fluorescent protein ubiquitously (Figure 2A), unless Cre-recombinase is expressed. By crossing with smooth muscle myosin heavy chain promoter–driven tamoxifen-inducible Cre-recombinase (SMMHC-Cre-ER) mice,[17] we specifically targeted the transgene to smooth muscle cells. All single-transgenic (STG) mice and Kir6.1 WT, GD, or GD-QR×SM-MHC-Cre double-transgenic (DTG) mice were viable and showed no obvious anatomical or behavioral pathology. Confocal images (Figure 2B) of cultured mesenteric artery smooth muscle cells isolated 3 weeks after induction show that the majority of myocytes from GD or GD-QR×Cre DTG mice lose green fluorescence but remain green in GD or GD-QR STG) mice (Figure 2B). Real-time PCR analysis (Figure 2C) shows that Kir6.1 mRNA level is significantly increased 12.6±4.5-fold in GD×SM-MHC-Cre DTG myocytes, and 7.5±1.8-fold in myocytes from GD-QR×SM-MHC-Cre DTG mice, compared with their STG littermates.

Kir6.1 GOF and LOF Transgenes Lead to Lower or Higher Blood Pressure, Respectively

Baseline heart rate and systolic, diastolic, and mean blood pressures were measured in anesthetized DTG and STG or WT littermates, 3 weeks following tamoxifen induction in smooth muscle. Both systolic and diastolic blood pressures were significantly lower in GD or GD-QR DTG compared with STG littermates (Figure 3A through 3C) but, importantly, blood pressure was not significantly affected in WT DTG compared with STG littermates (Figure 3D). Previous studies showed that total loss of Kir6.1 (or SUR2) function induced a Prinzmetal angina–like phenotype,[11,12] and although an elevated mean blood pressure was reported for the SUR2$^{-/-}$ animals, there was no report of overt hypertension in Kir6.1$^{-/-}$ animals. As additional controls for the present experiments, we also measured blood pressure from Kir6.1$^{-/-}$ mice[11] and from dominant-negative LOF Kir6.1[AAA] mice[12] crossed with SMMHC-Cre mice to target the transgene to the smooth muscle cells. Interestingly, blood pressure from both Kir6.1$^{-/-}$ and Kir6.1[AAA]×Cre-DTG mice was significantly higher than that of control WT or STG littermates (Figure 3E and 3F). As summarized in Figure 3G, this collection of mice represent a continuum of mean blood pressures ranging from <90% of control in GOF animals to >110% of control in LOF animals. Heart rates were not significantly different between groups,

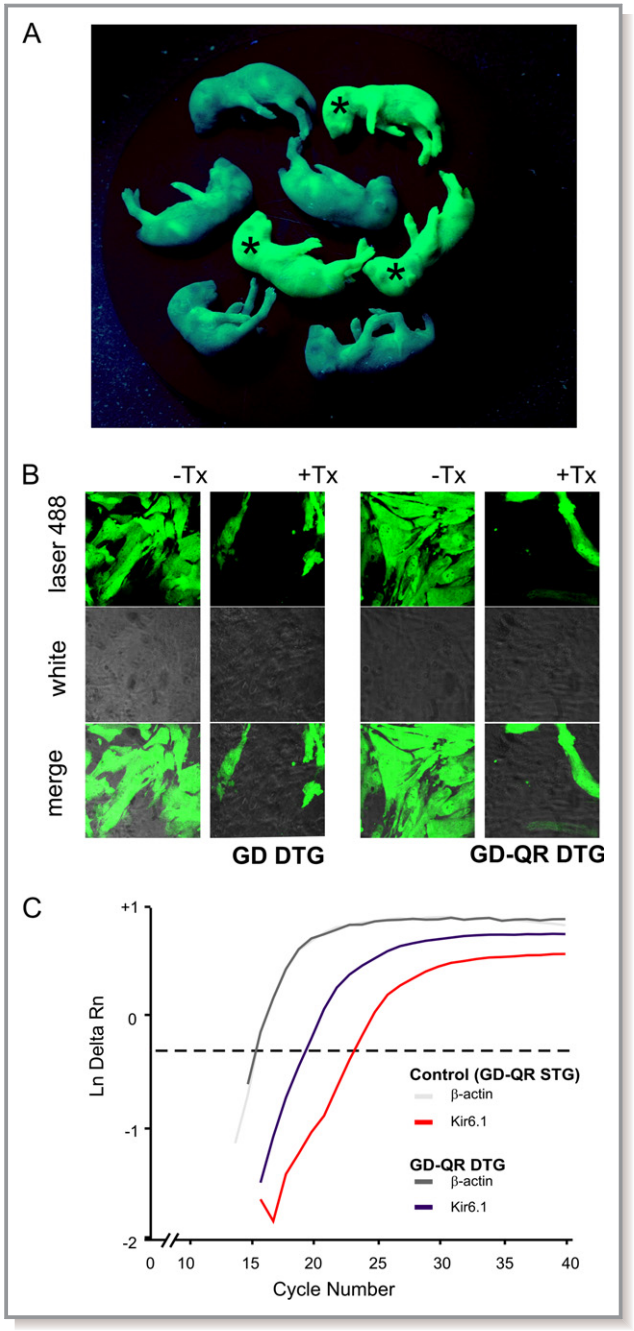

Figure 2. Generation of Cx1-Kir6.1[WT, GD, and GD-QR] transgenic mice, and targeted transgene expression in specific tissue. A, CX1 mice crossed with C57 WT mice, under UV light, newborn mice carrying the CX1 transgene were green (*), whereas nontransgenic mice were dark. B, Primary cultured mesenteric artery smooth muscle cells from the GD and GD-QR DTG offspring of CX1 transgenic mice and SMMHC-Cre-ER mice. Confocal images show that VSM cells from DTG with tamoxifen-induction lose green fluorescence but other cells remain green. C, In transgene targeted vascular tissue, quantitative real time PCR shows the copy number of transgene in DTG mice is significantly higher than that of their STG littermates. DTG indicates double-transgenic; PCR, polymerase chain reaction; SMMHC-Cre-ER, smooth muscle myosin heavy chain promoter-driven tamoxifen inducible Cre recombinase; STG, single-transgenic; VSM, vascular smooth muscle.

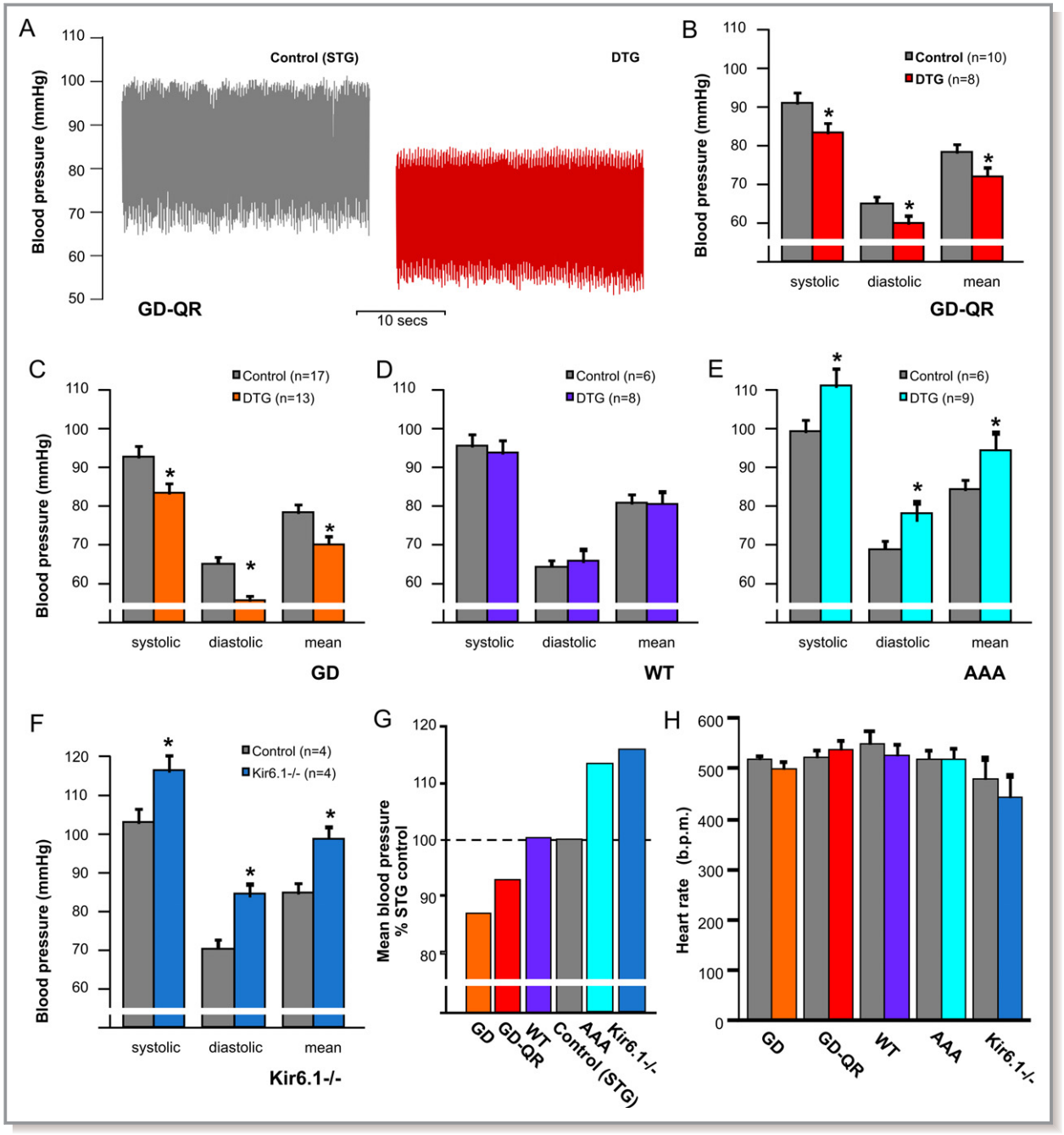

Figure 3. Kir6.1 GOF results in hypotension in mice, whereas Kir6.1 LOF results in hypertensive phenotype. A, Typical blood pressure measurement traces show that both systolic and diastolic blood pressure are markedly lower in anesthetized mice expressing GD-QR in smooth muscle cells than that of control littermates. B through F, Averaged systolic, diastolic, and mean blood pressures from each genotype studied in GD-QR (B), GD (C), WT (D) and AAA (E) DTG mice, and control littermates, as well as Kir6.1$^{-/-}$ and Kir6.1$^{+/+}$ littermates (F). *$P < .05$ versus control by unpaired Student's t tests in (B through F). G, Normalized averaged mean blood pressures of each genotype to the average value of their STG control littermates illustrates the marked progression from hypotensive GD and GD-QR DTG to hypertensive Kir6.1$^{-/-}$ and Kir6.1[AAA] animals. H, Heart rates from each condition demonstrate no significant difference by 1-way ANOVA. DTG indicates double-transgenic; GOF, gain-of-function; LOF, loss of function; WT, wild-type.

although we cannot exclude the possibility that insufficient sample size might mask small changes. As discussed earlier, transgenes were expressed at ≈10-fold higher levels than endogenous, at the mRNA level. Given the requisite stoichiometry between Kir6 and SUR subunits to generate functional K_{ATP} channels,[21] we expect that the net effect will be replacement of endogenous subunits with transgenic subunits in the surface channels, but we did not measure endogenous Kir6 or SUR mRNA or protein levels and cannot exclude the possibility that these may change. We also cannot know

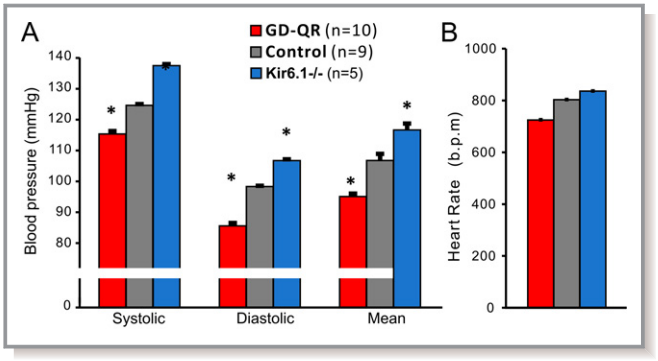

Figure 4. Kir6.1 GOF results in hypotension in conscious mice, whereas Kir6.1 LOF results in hypertensive phenotype (A) Averaged systolic, diastolic, and mean blood pressures from GD-QR DTG (n=10), Kir6.1$^{-/-}$ mice (n=5), and control mice (n=9). B, Averaged heart rates demonstrate no significant difference between the 3 groups. *$P < .05$ versus control by one-way ANOVA followed by post-hoc Tukey's test. DTG indicates double-transgenic; GOF, gain-of-function; LOF, loss of function.

whether excess subunits might bind to other proteins (other than regulatory SUR subunits), but the continuum of blood pressure responses, correlated with the expected effects of each genetic manipulation on physiological channel activity (and see below) is a strong argument against the possibility that level of Kir6 protein expression per se (or non-specific interactions with other proteins) underlies the effects on blood pressure.

Measurement of blood pressure in isoflurane-anesthetized animals may be of concern for several reasons. There is evidence that isoflurane can act as a K_{ATP} channel opener[22] which can provide a cardioprotective mechanism[23] and might preferentially activate K_{ATP} channels in GD and GD-QR DTG mice. More generally, anesthesia might produce confounding hemodynamic effects by altering baroreceptor function. We therefore also assessed blood pressure plethysmographically via tail cuff in conscious animals (Figure 4). These studies also reveal 10 to 15 mm Hg decrease in systolic and diastolic pressures in GD-QR DTG animals, and a corresponding increase in Kir6.1$^{-/-}$ mice, again without significant change of heart rate. The main concern for the use of plethysmography is that the animals must be restrained, which can lead to artifactually high pressure. Therefore, for these studies, the animals were trained daily for 2 weeks prior to recording. Importantly, the pressures in the control animals are consistent with measurements obtained by telemetry in conscious mice.[24,25]

Kir6.1 GOF Enhanced K_{ATP} Currents in Freshly Isolated Vascular Smooth Muscle Cells

To examine the effects of transgene expression on K_{ATP} channel activity in VSM membranes, we measured currents under whole-cell voltage-clamp in isolated single VSMCs from mesenteric arteries of transgenic mice and control littermates (Figure 5). Basal current in low (6 mmol/L) [K^+] was insignificant low (<1 pA/pF) in WT VSMCs (Figure 5A and 5C, control) but increased substantially when external [K^+] was elevated (to 140 mmol/L). Currents were further enhanced by the K_{ATP} channel opener pinacidil, and almost completely inhibited by glibenclamide, confirming that the basal high [K^+] current, as well as the pinacidil-activated current was through K_{ATP} channels. In GD DTG VSMCs, K^+ currents were higher than in WT VSMCs or VSMCs from STG littermates (Figure 5A and 5B) under all conditions, including basal, and significantly so in pinacidil. Conversely, there was no measurable K_{ATP} currents observed in VSMCs from Kir6.1$^{-/-}$ mice (Figure 5C and 5D).

Reduced Contractility but Normal Relaxation in Isolated Blood Vessels From Kir6.1 GOF Mice

The enhanced basal and pinacidil-activated currents in GD DTG myocytes are consistent with reduced excitability underlying reduced contractility and hence reduced blood pressures in the intact animal. To directly assess VSM contractility, vessel diameter was assessed in isolated mesenteric artery sections, in response to vasoactive agents (Figure 6). Contraction in response to phenylephrine (PE) was shifted ≈10-fold to higher [PE], in GD-QR DTG arteries compared with WT control arteries (Figure 6A and 6B) and an even greater relative shift was observed in the presence of the K_{ATP} channel opener-pinacidil (Figure 6B). Conversely, in the presence of glibenclamide, there was no statistical difference in response between the 2 genotypes (Figure 6B). The K_{ATP} specificity of this differential contractility is highlighted by the finding that following constriction by high [PE], subsequent K_{ATP}-independent relaxation in response to sodium nitroprusside was not different between the 2 genotypes.

Discussion

Kir6.1 Versus Kir6.2 in Native K_{ATP} Channel Complexes

Two genes, *KCNJ8* (Kir6.1) and *KCNJ11* (Kir6.2), encode K_{ATP} pore-forming subunits,[26,27] while 2 SUR genes, *ABCC8* (SUR1) *and ABCC9* (SUR2), generate regulatory subunits[28,29] of K_{ATP} channels. Kir6.1 and Kir6.2 confer distinct biochemical and biophysical properties on the octameric channel complex, with Kir6.1 channels exhibiting a marked requirement for Mg-nucleotide activation (Figure 1B) and being of lower conductance.[5] While Kir6.2 is an obligatory subunit in skeletal and cardiac muscle K_{ATP} channels, and prominent in pancreatic and neuronal K_{ATP} channels, Kir6.1 is generally absent from these tissues but is widely expressed throughout the vasculature.[30] Accordingly, LOF mutations in Kir6.2 result in hypoglycemia

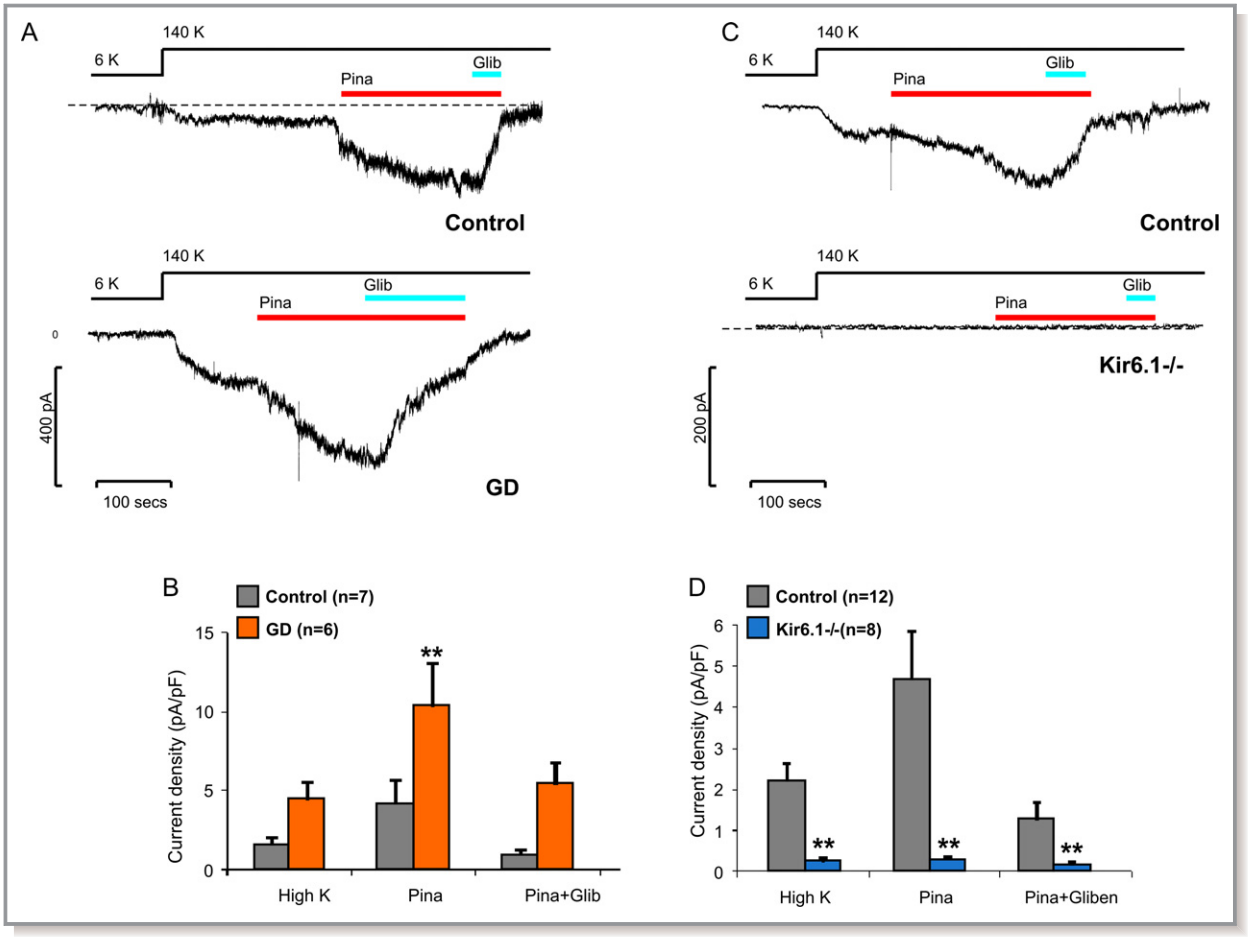

Figure 5. Kir6.1 GOF results in enhanced K_{ATP} channel currents in isolated arterial smooth muscle cells. A and C, Representative whole-cell recordings of K_{ATP} currents in control (top) and GD DTG (A) or Kir6.1$^{-/-}$ (C) (bottom) VSMCs. VSMCs were sequentially exposed to low (6 mmol/L) K^+, high (140 mmol/L) K^+, pinacidil, and glibenclamide. B and D, Summarized data show K_{ATP} current density in high K^+, pinacidil and glibenclamide for GD DTG (B) or Kir6.1$^{-/-}$ (D) and control littermate VSMCs. $^{**}P < .01$ versus control at the same condition, by 2-way ANOVA followed by Bonferroni's posttests. DTG indicates double-transgenic; GOF, gain-of-function; VSMCs, vascular smooth muscle cells.

and hyperinsulinemia, whereas Kir6.2 GOF mutations result in pancreatic β-cell underactivity and neonatal diabetes.[9,10] In mice, deletion of Kir6.1 results in spontaneous coronary vasospasm and a Prinzmetal angina–like phenotype,[11] but the consequences of overactivity of Kir6.1 in vivo are unknown. Given the high sequence homology between Kir6.1 and Kir6.2, we hypothesized that the GOF mutations in Kir6.1 that are homologous to neonatal diabetes–causing Kir6.2 mutations will cause pathology in mice and that these consequences might parallel the relevant human diseases.

Certain disease-causing GOF Kir6.2 mutations (eg, Gly334 Asp[19]) are located in the ATP binding site and alter ATP-sensitivity directly, whereas others (eg, Gln52Arg[20]) are located outside the binding pocket and alter ATP-sensitivity indirectly, by altering intrinsic gating of the channel. We show that when engineered at homologous residues in Kir6.1 (Gly343Asp and Gln53Arg) (Figure 1A), each of the equivalent mutations cause loss of ATP inhibition (Figure 1B and 1C) and increased channel activity in the intact cell (Figure 1D). These data confirm the structure–function correlation between Kir6.1 and Kir6.2 and establish that ATP inhibition is similarly sensitive to specific mutations in the ATP-binding site and gating regions, thereby providing the critical rationale to engineer Kir6.1 GOF in vivo.

Kir6.1 in Vascular Smooth Muscle K_{ATP}

Kir6.1 expression has been reported in numerous tissues, prominently throughout the vasculature, although there is evidence of variable biophysical and pharmacological properties in different VSM types, which likely reflect differential expression of different subunits in vascular beds.[2,31] Low-conductance channels (unitary conductances from 20 to 50 pS), which are inactive in isolated membrane patches and which require nucleoside diphosphates (ADP, UDP, GDP) in the presence of Mg^{2+} to open,[31,32] are predominant and are likely to reflect Kir6.1 subunits (Figure 1B).[5,33]

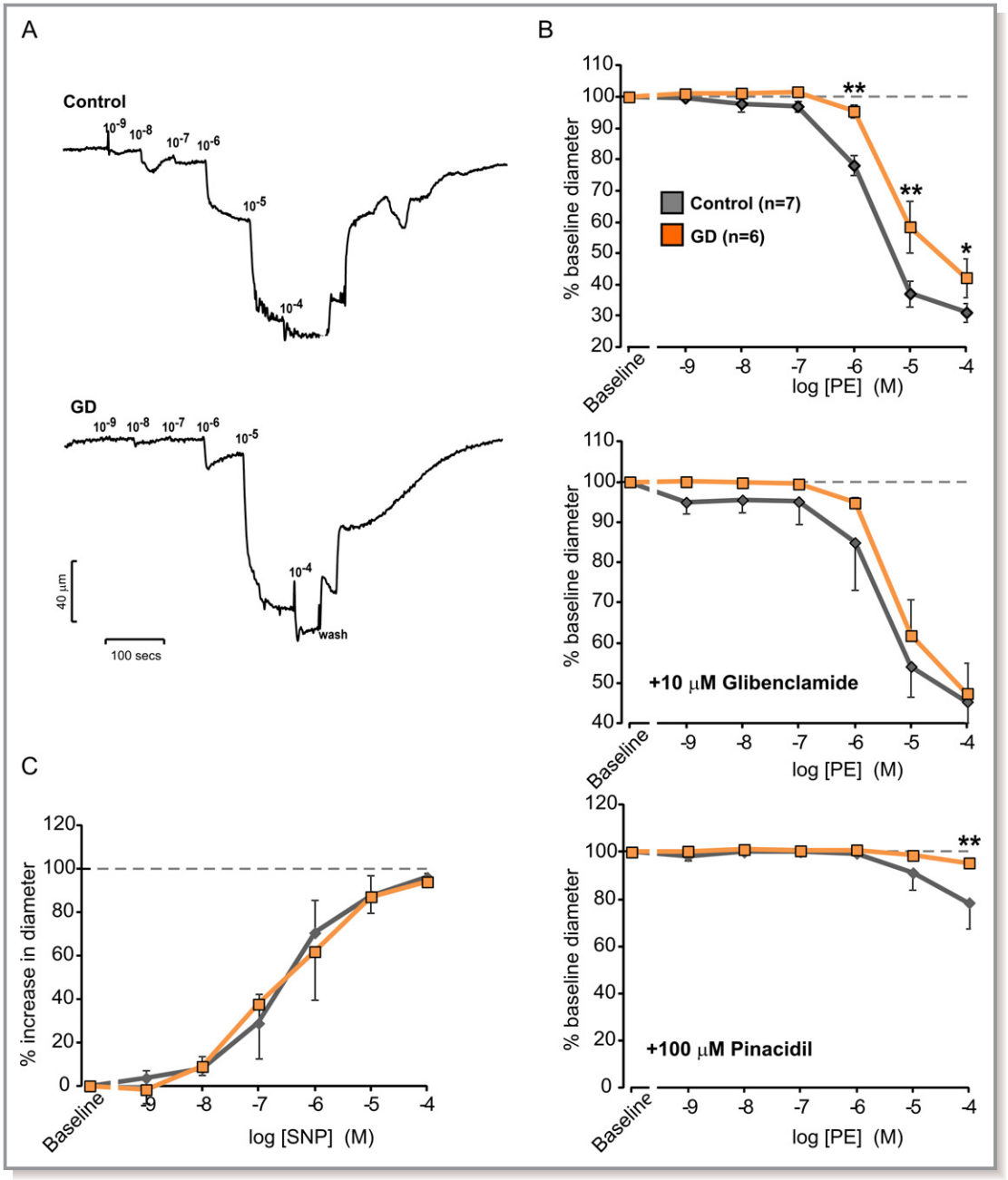

Figure 6. Kir6.1 GOF results in decreased vascular reactivity of Kir6.1 GOF mouse mesenteric arteries. A, Representative recordings of vessel diameter of (top) WT control and GD-QR DTG (bottom) mesenteric arteries in response to increasing phenylephrine (PE) concentrations. B, Concentration-response of PE-induced vasoconstriction from experiments as in (A) (n=6 in each case) expressed as percent decrease in arterial diameter after application of each concentration of PE (10^{-9} to 10^{-4} mmol/L) as indicated (top) and in the additional presence of glibenclamide 10 μmol/L (center) or pinacidil 100 μmol/L (bottom). C, Concentration-dependent vasodilatation of control and GD-QR DTG mesenteric arteries in response to sodium nitroprusside (SNP) following constriction with 5 μmol/L PE. As indicated, percent relaxation shows no difference between control (n=4) and GD-QR DTG (n=5) arterial diameter after application of PE and increasing concentration of SNP. Data are expressed as mean±SE in all cases. *$P < .05$, **$P < .01$ versus control at the same condition (2-way repeated-measures ANOVA followed by Bonferroni's posttests). DTG indicates double-transgenic; GOF, gain-of-function; WT, wild-type.

K_{ATP} currents are reportedly normal in aortic smooth muscle myocytes from Kir6.2$^{-/-}$ mice.[11,34] Here we show that K_{ATP} currents are significantly increased in VSMCs from GD mice but absent in Kir6.1$^{-/-}$ VSMCs (Figure 4C and 4D). These data confirm the essential requirement for Kir6.1 subunits in pinacidil- and glibenclamide-sensitive K_{ATP} currents in aortic smooth muscle. The current data also show that expression of GD subunits increases basal K_{ATP} currents more obviously than pinacidil-activated currents, reflecting loss of ATP sensitivity in GD and suggesting that basal activity

of channels will be present in these VSMCs in vivo. It is also noteworthy that glibenclamide inhibition of these currents is less than the glibenclamide inhibition of WT channels, again reflective of the loss of sulfonylurea sensitivity documented for the open-state stabilizing Gln52Asp mutation in Kir6.2.[20]

Vascular K_{ATP} and Blood Pressure Control

K_{ATP} channels are presumed to be tonically active in many vascular beds, and hence to play a role in establishing basal vessel tone, based on glibenclamide-induced depolarization and constriction, both in isolated arteries and in vivo.[35] Pharmacological activation of K_{ATP} channels typically leads to a lowering of intracellular Ca^{2+} levels, increase in arteriole diameter, and decrease in vascular resistance,[2] but the exact target of such activators is not always clear. For instance, there is controversy regarding the role of K_{ATP} channels in smooth muscle versus channels in endothelium,[36] and there is significant controversy regarding the action of K_{ATP} drugs on mitochondrial versus surface membrane channels.[30] Spontaneous coronary vasospasm and a Prinzmetal angina–like phenotype that results from deletion of Kir6.1[11] or SUR2[11,13] presumably reflect a normal role of channels formed from these subunits somewhere in the vasculature, potentially in smooth muscle, although restoration of WT SUR2B expression in the latter case does not appear to rescue the phenotype,[36] implicating a smooth muscle extrinsic mechanism. Lower currents in glibenclamide compared with high K^+ alone in control VSMCs (Figure 4) indicates some basal activity of these channels in isolated control VSMCs. Gain of K_{ATP} channel activity is therefore predicted to cause a relative hyperpolarization of the membrane potential, inhibition of L-type voltage-sensitive Ca^{2+}-channels, Ca^{2+} entry, accounting for the observed vasorelaxation and lowering of blood pressure in ATP-insensitive GD DTG or GD-QR DTG mice. Consistent with elevated basal K_{ATP} channel activity in GD-QR GOF mesenteric arteries, we showed ≈10-fold shift in the PE dependence of vessel contraction compared with WT controls (Figure 6), which was absent in the presence of glibenclamide and exacerbated in the presence of pinacidil (Figure 6). Importantly, the blood pressure of WT/Cre-DTG mice remained normal (Figure 3D), arguing that blood pressure lowering in GD/Cre-DTG and GD-QR/Cre-DTG is a result of reduced K_{ATP} channel ATP sensitivity and arguing against a simple effect of overexpression of Kir6.1 subunits. In addition, a recent study shows that overexpression of the K_{ATP} channel Kir6.2 subunit does not affect endogenous SUR subunit mRNA levels in mice,[37] such that overexpression of the Kir6 subunit per se will not alter SUR subunit levels, which may limit the overall K_{ATP} channel density.

The data are entirely consistent with the introduced GOF mutant channels causing primary hypotension. Although previous studies did not report effects of total or partial loss of Kir6.1 function on systemic blood pressures,[11,12] the current data, examining littermate controls, indicate that knockout of Kir6.1 or expression of dominant-negative Kir6.1 [AAA] in VSM increase both systolic and diastolic pressures (Figures 3 and 4), again consistent with basal K_{ATP} channel activity being normally present in WT vessels. The direct hyperpolarizing effects of ATP-insensitive Kir6.1 on VSM can explain depressed vasoconstrictor responsiveness and consequent hypotension. It might be expected that the renin-angiotensin system or baroreceptor reflexes might counter the hypotension. Little is known about the relative efficacy of the renin-angiotensin system in rodents versus humans, and it remains to be seen whether there is in fact any partial compensation through such mechanisms.

Genetic Alterations of Cardiovascular K_{ATP} in Humans: Cantu Syndrome

Knockout animals have been generated for each of the 4 K_{ATP} subunit genes.[30] These animals have established that distinct pairs form native channels in different tissues. Both SUR1 and Kir6.2 knockouts reiterate a glucose-insensitive insulin secretory phenotype due to loss of K_{ATP} in the pancreas.[7,38,39] GOF Kir6.2 mutants in the pancreas cause severe neonatal diabetes in mice[10] and humans.[9] Expression of GOF Kir6.2 subunits in cardiac myocytes is well tolerated with minimal effect on heart function,[40,41] but again mimicking and predicting the benign cardiac phenotype in neonatal diabetes.[42] Thus, while SUR1 and Kir6.2 mutations clearly cause human disease through alterations of pancreatic function, it has not been obvious what the pathological consequences of Kir6.1 or SUR2 mutations will be in humans. Murine Kir6.1 and SUR2 knockouts reiterate a phenotype mimicking human Prinzmetal angina,[11,13] with spontaneous coronary vasospasm leading to early death. Until now, the only Kir6.1 transgenic animals that have been generated express dominant-negative Kir6.1[AAA] subunit under tamoxifen-Cre control and have been targeted only to cardiac myocytes[43] or to endothelium.[12] The latter animals had no overt phenotype and no early mortality, but there was an elevated basal coronary perfusion pressure in isolated hearts, suggesting a role for endothelium-expressed Kir6.1 in control of vascular tone, potentially via elevated endothelin-1 release. Our present demonstration that smooth muscle Kir6.1 LOF and GOF, respectively, cause overt hypertension and hypotension suggests that similar human pathologies might be expected from Kir6.1 mutations. Intriguingly, the Kir6.1 and SUR2 genes are located on human chromosome 12p; chromosome 12p recombination has been shown to underlie autosomal dominant hypertension,[44] and postural hypotension is linked to chromosome 12.[45] Although our recent analysis of Kir6.1 and SUR2 genes in a cohort of such patients failed to reveal

any associated variants,[46] further investigation may be warranted.

Strikingly, 2 recent studies showed conclusively that Cantu syndrome results from SUR2 GOF mutations in humans.[47,48] Cantu syndrome (MIM 239850) is a complex multiorgan disease characterized by congenital hypertrichosis, edema, macrocephaly, dysmorphic features, skeletal abnormalities, and generalized osteopenia, as well as multiple additional clinical features. Cardiovascular features include cardiac hypertrophy, pulmonary hypertension, and pericardial effusion. A significant number of patients have had patent ductus arteriosus requiring surgical closure, as well as bicuspid aortic valve with and without stenosis. Marked edema involving the lower extremities may develop over time, and in 1 patient, lymphangiogram demonstrated dilated lymphatic vessels in the legs with delayed lymphatic drainage.[49] Previous studies of Cantu syndrome patients provided no definitive explanation of the underlying cause of the various features, and even now the realization of SUR2 mutations as causal does not immediately provide explanations for all features. The K_{ATP} channel openers diazoxide and minoxidil have been used since the 1960s to treat severe refractory hypertension, and multiple side effects of these drugs include pronounced hypertrichosis, pericardial effusions, and edema. Teratogenic effects of minoxidil, including marked hypertrichosis, dysmorphic facial features, and low blood pressure, have been reported in the offspring of a minoxidil-treated mother.[50] Overt hypotension has not been reported in adult Cantu syndrome patients, but edema, pericardial effusion, and patent ductus arteriosus may all point to excessive vascular relaxation. After birth, the abrupt increase in oxygen tension and falling prostaglandin E_2 and I_2 levels lead to inhibition of voltage-gated K channels and contraction of smooth muscle fibers in the ductus, resulting in wall thickening and lumen obliteration. Enhancement of K_{ATP} current in the vessel smooth muscle presents an obvious potential explanation for excessive patent ductus arteriosus in Cantu syndrome.

These new analyses of Cantu syndrome patients focused on the SUR2 (*ABCC9*) gene and uncovered coding mutations in 25 of 31 patients, but this still leaves 6 of these patients unaccounted for. Given our findings, GOF mutations in Kir6.1 remain possible candidate causes. It should be pointed out that several recent studies have reported a mutation, Ser422Lys, in the Kir6.1 protein to be associated with the "J-wave" phenomenon, characterized by abnormalities in the J-point of the ECG.[14,16] As part of the original study,[14] we failed to detect any alteration in the properties of Ser422Lys variant Kir6.1/SUR2A currents in recombinant cells (J.C. Koster, PhD, and C.G. Nichols, PhD, unpublished data), but the later studies have reported enhanced channel activity for the Ser422Lys variant, arguing that GOD in Kir6.1 channel activity is underlying the ERS and hence atrial fibrillation (AF). How this occurs will require further examination, and the animals that we have generated in the present study may be useful in this regard. The results of the present study specifically illuminate the role of Kir6.1 GOF in VSM, but with appropriate crosses, these animals may also be used to test the role of Kir6.1 in endothelium, as well as cardiac muscle and other tissues.

Acknowledgments

We greatly appreciate the assistance of Mark Knuepfer (Saint Louis University) in obtaining blood pressure measurements and for important insights and comments on early drafts of the manuscript.

Sources of Funding

This work was supported by National Institutes of Health (NIH) grant (HL45742 to Dr Nichols) and an American Heart Association grant-in-aid (to Dr Koster), as well as NIH grants (NS071011, HL041250) and Barnes-Jewish/Christian Foundation (to Dr Dietrich).

Disclosures

None.

References

1. Noma A. ATP-regulated K^+ channels in cardiac muscle. *Nature*. 1983;305:147–148.
2. Standen NB, Quayle JM, Davies NW, Brayden JE, Huang Y, Nelson MT. Hyperpolarizing vasodilators activate ATP-sensitive K^+ channels in arterial smooth muscle. *Science*. 1989;245:177–180.
3. Katnik C, Adams DJ. Characterization of ATP-sensitive potassium channels in freshly dissociated rabbit aortic endothelial cells. *Am J Physiol*. 1997;272:H2507–H2511.
4. Kurata HT, Marton LJ, Nichols CG. The polyamine binding site in inward rectifier K^+ channels. *J Gen Physiol*. 2006;127:467–480.
5. Yamada M, Isomoto S, Matsumoto S, Kondo C, Shindo T, Horio Y, Kurachi Y. Sulphonylurea receptor 2B and Kir6.1 form a sulphonylurea-sensitive but ATP-insensitive K^+ channel. *J Physiol*. 1997;499:715–720.
6. Seino S, Miki T. Gene targeting approach to clarification of ion channel function: studies of Kir6.x null mice. *J Physiol*. 2004;554:295–300.
7. Miki T, Nagashima K, Tashiro F, Kotake K, Yoshitomi H, Tamamoto A, Gonoi T, Iwanaga T, Miyazaki J, Seino S. Defective insulin secretion and enhanced insulin action in KATP channel-deficient mice. *Proc Natl Acad Sci USA*. 1998;95:10402–10406.
8. Koster JC, Remedi MS, Flagg TP, Johnson JD, Markova KP, Marshall BA, Nichols CG. Hyperinsulinism induced by targeted suppression of beta cell KATP channels. *Proc Natl Acad Sci USA*. 2002;99:16992–16997.
9. Gloyn AL, Pearson ER, Antcliff JF, Proks P, Bruining GJ, Slingerland AS, Howard N, Srinivasan S, Silva JM, Molnes J, Edghill EL, Frayling TM, Temple IK, Mackay D, Shield JP, Sumnik Z, van Rhijn A, Wales JK, Clark P, Gorman S, Aisenberg J, Ellard S, Njolstad PR, Ashcroft FM, Hattersley AT. Activating mutations in the gene encoding the ATP-sensitive potassium-channel subunit Kir6.2 and permanent neonatal diabetes. *N Engl J Med*. 2004;350:1838–1849.
10. Koster JC, Marshall BA, Ensor N, Corbett JA, Nichols CG. Targeted overactivity of beta cell K(ATP) channels induces profound neonatal diabetes. *Cell*. 2000;100:645–654.
11. Miki T, Suzuki M, Shibasaki T, Uemura H, Sato T, Yamaguchi K, Koseki H, Iwanaga T, Nakaya H, Seino S. Mouse model of Prinzmetal angina by disruption of the inward rectifier Kir6.1. *Nat Med*. 2002;8:466–472.
12. Malester B, Tong X, Ghiu I, Kontogeorgis A, Gutstein DE, Xu J, Hendricks-Munoz KD, Coetzee WA. Transgenic expression of a dominant negative

K(ATP) channel subunit in the mouse endothelium: effects on coronary flow and endothelin-1 secretion. *FASEB J*. 2007;21:2162–2172.

13. Chutkow WA, Pu J, Wheeler MT, Wada T, Makielski JC, Burant CF, McNally EM. Episodic coronary artery vasospasm and hypertension develop in the absence of Sur2 K(ATP) channels [see comment]. *J Clin Invest*. 2002;110:203–208.
14. Haissaguerre M, Chatel S, Sacher F, Weerasooriya R, Probst V, Loussouarn G, Horlitz M, Liersch R, Schulze-Bahr E, Wilde A, Kaab S, Koster J, Rudy Y, Le Marec H, Schott JJ. Ventricular fibrillation with prominent early repolarization associated with a rare variant of KCNJ8/KATP channel. *J Cardiovasc Electrophysiol*. 2009;20:93–98.
15. Barajas-Martinez H, Hu D, Ferrer T, Onetti CG, Wu Y, Burashnikov E, Boyle M, Surman T, Urrutia J, Veltmann C, Schimpf R, Borggrefe M, Wolpert C, Ibrahim BB, Sanchez-Chapula JA, Winters S, Haissaguerre M, Antzelevitch C. Molecular genetic and functional association of Brugada and early repolarization syndromes with S422L missense mutation in KCNJ8. *Heart Rhythm*. 2012;9:548–555.
16. Medeiros-Domingo A, Tan BH, Crotti L, Tester DJ, Eckhardt L, Cuoretti A, Kroboth SL, Song C, Zhou Q, Kopp D, Schwartz PJ, Makielski JC, Ackerman MJ. Gain-of-function mutation S422L in the KCNJ8-encoded cardiac K(ATP) channel Kir6.1 as a pathogenic substrate for J-wave syndromes. *Heart Rhythm*. 2010;7:1466–1471.
17. Regan CP, Manabe I, Owens GK. Development of a smooth muscle-targeted cre recombinase mouse reveals novel insights regarding smooth muscle myosin heavy chain promoter regulation. *Circ Res*. 2000;87:363–369.
18. Bernal-Mizrachi C, Xiaozhong L, Yin L, Knutsen RH, Howard MJ, Arends JJ, Desantis P, Coleman T, Semenkovich CF. An afferent vagal nerve pathway links hepatic PPARalpha activation to glucocorticoid-induced insulin resistance and hypertension. *Cell Metab*. 2007;5:91–102.
19. Masia R, Koster JC, Tumini S, Chiarelli F, Colombo C, Nichols CG, Barbetti F. An ATP-binding mutation (G334D) in KCNJ11 is associated with a sulfonylurea-insensitive form of developmental delay, epilepsy, and neonatal diabetes. *Diabetes*. 2007;56:328–336.
20. Koster JC, Remedi MS, Dao C, Nichols CG. ATP and sulfonylurea sensitivity of mutant ATP-sensitive K^+ channels in neonatal diabetes: implications for pharmacogenomic therapy. *Diabetes*. 2005;54:2645–2654.
21. Nichols C. KATP channels as molecular sensors of cellular metabolism. *Nature*. 2006;440:470–476.
22. Han J, Kim E, Ho WK, Earm YE. Effects of volatile anesthetic isoflurane on ATP-sensitive K^+ channels in rabbit ventricular myocytes. *Biochem Biophys Res Commun*. 1996;229:852–856.
23. Tonkovic-Capin M, Gross GJ, Bosnjak ZJ, Tweddell JS, Fitzpatrick CM, Baker JE. Delayed cardioprotection by isoflurane: role of K(ATP) channels. *Am J Physiol Heart Circ Physiol*. 2002;283:H61–H68.
24. Brockway BP, Mills PA, Azar SH. A new method for continuous chronic measurement and recording of blood pressure, heart rate and activity in the rat via radio-telemetry. *Clin Exp Hypertens A*. 1991;13:885–895.
25. Fryer RM, Rakestraw PA, Banfor PN, Cox BF, Opgenorth TJ, Reinhart GA. Blood pressure regulation by ETA and ETB receptors in conscious, telemetry-instrumented mice and role of ETA in hypertension produced by selective ETB blockade. *Am J Physiol Heart Circ Physiol*. 2006;290:H2554–H2559.
26. Inagaki N, Gonoi T, Clement JP, Wang CZ, Aguilar-Bryan L, Bryan J, Seino S. A family of sulfonylurea receptors determines the pharmacological properties of ATP-sensitive K^+ channels. *Neuron*. 1996;16:1011–1017.
27. Inagaki N, Gonoi T, Clement JP IV, Namba N, Inazawa J, Gonzalez G, Aguilar-Bryan L, Seino S, Bryan J. Reconstitution of IKATP: an inward rectifier subunit plus the sulfonylurea receptor [see comments]. *Science*. 1995;270:1166–1170.
28. Aguilar-Bryan L, Nichols CG, Wechsler SW, Clement JP IV, Boyd AE III, Gonzalez G, Herrera-Sosa H, Nguy K, Bryan J, Nelson DA. Cloning of the beta cell high-affinity sulfonylurea receptor: a regulator of insulin secretion. *Science*. 1995;268:423–426.
29. Chutkow WA, Simon MC, Le Beau MM, Burant CF. Cloning, tissue expression, and chromosomal localization of SUR2, the putative drug-binding subunit of cardiac, skeletal muscle, and vascular KATP channels. *Diabetes*. 1996;45:1439–1445.
30. Flagg TP, Enkvetchakul D, Koster JC, Nichols CG. Muscle KATP channels: recent insights to energy sensing and myoprotection. *Physiol Rev*. 2010;90:799–829.
31. Beech DJ, Zhang H, Nakao K, Bolton TB. K channel activation by nucleotide diphosphates and its inhibition by glibenclamide in vascular smooth muscle cells. *Br J Pharmacol*. 1993;110:573–582.
32. Zhang HL, Bolton TB. Two types of ATP-sensitive potassium channels in ratportal vein smooth muscle cells. *Br J Pharmacol*. 1996;118:105–114.
33. Babenko AP, Bryan J. A conserved inhibitory and differential stimulatory action of nucleotides on K(IR)6.0/SUR complexes is essential for excitation-metabolism coupling by K(ATP) channels. *J Biol Chem*. 2001;276:49083–49092.
34. Suzuki M, Li RA, Miki T, Uemura H, Sakamoto N, Ohmoto-Sekine Y, Tamagawa M, Ogura T, Seino S, Marban E, Nakaya H. Functional roles of cardiac and vascular ATP-sensitive potassium channels clarified by Kir6.2-knockout mice. *Circ Res*. 2001;88:570–577.
35. Nelson MT, Huang Y, Brayden JE, Hescheler J, Standen NB. Arterial dilations in response to calcitonin gene-related peptide involve activation of K^+ channels. *Nature*. 1990;344:770–773.
36. Kakkar R, Ye B, Stoller DA, Smelley M, Shi NQ, Galles K, Hadhazy M, Makielski JC, McNally EM. Spontaneous coronary vasospasm in KATP mutant mice arises from a smooth muscle-extrinsic process [see comment]. *Circ Res*. 2006;98:682–689.
37. Clark RH, McTaggart JS, Webster R, Mannikko R, Iberl M, Sim XL, Rorsman P, Glitsch M, Beeson D, Ashcroft FM. Muscle dysfunction caused by a KATP channel mutation in neonatal diabetes is neuronal in origin. *Science*. 2010;329:458–461.
38. Seghers V, Nakazaki M, DeMayo F, Aguilar-Bryan L, Bryan J. Sur1 knockout mice. A model for K(ATP) channel-independent regulation of insulin secretion. *J Biol Chem*. 2000;275:9270–9277.
39. Shiota C, Larsson O, Shelton KD, Shiota M, Efanov AM, Hoy M, Lindner J, Kooptiwut S, Juntti-Berggren L, Gromada J, Berggren PO, Magnuson MA. Sulfonylurea receptor type 1 knock-out mice have intact feeding-stimulated insulin secretion despite marked impairment in their response to glucose. *J Biol Chem*. 2002;277:37176–37183.
40. Koster JC, Knopp A, Flagg TP, Markova KP, Sha Q, Enkvetchakul D, Betsuyaku T, Yamada KA, Nichols CG. Tolerance for ATP-insensitive K(ATP) channels in transgenic mice. *Circ Res*. 2001;89:1022–1029.
41. Masia R, Enkvetchakul D, Nichols C. Differential nucleotide regulation of K(ATP) channels by SUR1 and SUR2A. *J Mol Cell Cardiol*. 2005;39:491–501.
42. Tammaro P, Girard C, Molnes J, Njolstad PR, Ashcroft FM. Kir6.2 mutations causing neonatal diabetes provide new insights into Kir6.2-SUR1 interactions. *EMBO J*. 2005;24:2318–2330.
43. Tong X, Porter LM, Liu G, Dhar-Chowdhury P, Srivastava S, Pountney DJ, Yoshida H, Artman M, Fishman GI, Yu C, Iyer R, Morley GE, Gutstein DE, Coetzee WA. Consequences of cardiac myocyte-specific ablation of KATP channels in transgenic mice expressing dominant negative Kir6 subunits. *Am J Physiol Heart Circ Physiol*. 2006;291:H543–H551.
44. Bahring S, Rauch A, Toka O, Schroeder C, Hesse C, Siedler H, Fesus G, Haefeli WE, Busjahn A, Aydin A, Neuenfeld Y, Muhl A, Toka HR, Gollasch M, Jordan J, Luft FC. Autosomal-dominant hypertension with type E brachydactyly is caused by rearrangement on the short arm of chromosome 12. *Hypertension*. 2004;43:471–476.
45. Harrap SB, Cui JS, Wong ZY, Hopper JL. Familial and genomic analyses of postural changes in systolic and diastolic blood pressure. *Hypertension*. 2004;43:586–591.
46. Ellis JA, Lamantia A, Chavez R, Scurrah KJ, Nichols CG, Harrap SB. Genes controlling postural changes in blood pressure: comprehensive association analysis of ATP-sensitive potassium channel genes KCNJ8 and ABCC9. *Physiol Genomics*. 2009;40:184–188.
47. van Bon BW, Gilissen C, Grange DK, Hennekam RC, Kayserili H, Engels H, Reutter H, Ostergaard JR, Morava E, Tsiakas K, Isidor B, Le Merrer M, Eser M, Wieskamp N, de Vries P, Steehouwer M, Veltman JA, Robertson SP, Brunner HG, de Vries BB, Hoischen A. Cantu syndrome is caused by mutations in ABCC9. *Am J Hum Genet*. 2012;90:1094–1101.
48. Harakalova M, van Harssel JJ, Terhal PA, van Lieshout S, Duran K, Renkens I, Amor DJ, Wilson LC, Kirk EP, Turner CL, Shears D, Garcia-Minaur S, Lees MM, Ross A, Venselaar H, Vriend G, Takanari H, Rook MB, van der Heyden MA, Asselbergs FW, Breur HM, Swinkels ME, Scurr IJ, Smithson SF, Knoers NV, van der Smagt JJ, Nijman IJ, Kloosterman WP, van Haelst MM, van Haaften G, Cuppen E. Dominant missense mutations in ABCC9 cause Cantu syndrome. *Nat Genet*. 2012;44:793–796.
49. Garcia-Cruz D, Mampel A, Echeverria MI, Vargas AL, Castaneda-Cisneros G, Davalos-Rodriguez N, Patino-Garcia B, Garcia-Cruz MO, Castaneda V, Cardona EG, Marin-Solis B, Cantu JM, Nunez-Reveles N, Moran-Moguel C, Thavanati PK, Ramirez-Garcia S, Sanchez-Corona J. Cantu syndrome and lymphoedema. *Clin Dysmorphol*. 2011;20:32–37.
50. Kaler SG, Patrinos ME, Lambert GH, Myers TF, Karlman R, Anderson CL. Hypertrichosis and congenital anomalies associated with maternal use of minoxidil. *Pediatrics*. 1987;79:434–436.